ACS APPLIED MATERIALS & INTERFACES

Research Article

www.acsami.org

Nanostructured Donor–Acceptor Self Assembly with Improved Photoconductivity

B. Saibal,[†,§] A. Z. Ashar,[⊥] R. Nandini Devi,[‡,§] K. S. Narayan,*[,⊥] and S. K. Asha*[,†,§,∥]

[†]Polymer Science and Engineering Division, [‡]Catalysis & Inorganic Chemistry Division, CSIR-National Chemical Laboratory, Dr. Homi Bhabha Road, Pune 411008, India

[§]Academy of Scientific and Innovative Research, New Delhi 110025, India

[∥]CSIR-Network Institutes of Solar Energy, New Delhi 110001, India

[⊥]Chemistry and Physics of Material Unit, Jawaharlal Nehru Centre for Advanced Scientific Research Jakkur, Bangalore 560064, Karnataka, India

Supporting Information

ABSTRACT: Nanostructured supramolecular donor–acceptor assemblies were formed when an unsymmetrical N-substituted pyridine functionalized perylenebisimide (UPBI-Py) was complexed with oligo(*p*-phenylenevinylene) (OPVM-OH) complementarily functionalized with hydroxyl unit and polymerizable methacrylamide unit at the two termini. The resulting supramolecular complex [UPBI-Py (OPVM-OH)]$_{1.0}$ upon polymerization by irradiation in the presence of photoinitiator formed well-defined supramolecular polymeric nanostructures. Self-assembly studies using fluorescence emission from thin film samples showed that subtle structural changes occurred on the OPV donor moiety following polymerization. The 1:1 supramolecular complex showed red-shifted aggregate emission from both OPV (~500 nm) and PBI (~640 nm) units, whereas the OPV aggregate emission was replaced by intense monomeric emission (~430 nm) upon polymerizing the methacrylamide units on the OPVM-OH. The bulk structure was studied using wide-angle X-ray diffraction (WXRD). Complex formation resulted in distinct changes in the cell parameters of OPVM-OH. In contrast, a physical mixture of 1 mol each of OPVM-OH and UPBI-Py prepared by mixing the powdered solid samples together showed only a combination of reflections from both parent molecules. Thin film morphology of the 1:1 molecular complex as well as the supramolecular polymer complex showed uniform lamellar structures in the domain range <10 nm. The donor–acceptor supramolecular complex [UPBI-Py (OPVM-OH)]$_{1.0}$ exhibited space charge limited current (SCLC) with a bulk mobility estimate of an order of magnitude higher accompanied by a higher photoconductivity yield compared to the pristine UPBI-Py. This is a very versatile method to obtain spatially defined organization of n and p-type semiconductor materials based on suitably functionalized donor and acceptor molecules resulting in improved photocurrent response using self-assembly.

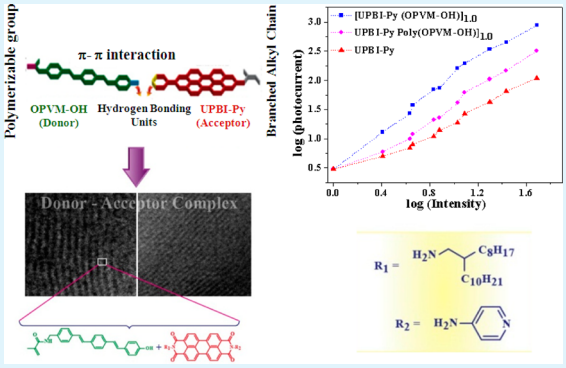

KEYWORDS: *hydrogen bonding, perylenebisimide, oligo(p-phenylenevinylene), donor–acceptor, photoconductivity, supramolecular polymeric nanostructures*

INTRODUCTION

The bottom-up self-assembly of donor–acceptor semiconducting materials is a very challenging task that is being pursued by researchers worldwide.[1−8] Well-defined and reproducible nanoscale assemblies of donor–acceptor semiconducting materials are crucial for several devices in the optoelectronic applications.[1−4] From the perspective of device applications, it is highly desirable to translate the self-assembly of small molecules to processable polymers, which is a nontrivial task. A promising approach in this regard has been the one pioneered by the group of Ikkala and ten Brinke et. al to form hierarchical architectures of small surfactant molecules with block copolymers.[9−12] Recently, we reported well-defined nanoorganization of n-type semiconductors based on perylenebisimide with the polymer poly(4-vinylpyridine) (P4VP), resulting in lamellar structures in the domain range 5−10 nm with a clear trend of higher conductance compared to the pristine PBI molecule.[13] Ting Xu and Fréchet et al. attached suitably functionalized p-type organic semiconductor - oligothiophene to P4VP resulting in solution processable nanostructured semiconductor composites with charge carrier mobilities comparable to the existing semiconductors already used in OPV devices.[14,15] Both these approaches took aid of the self-assembly afforded by the nanoscale phase separation of the

Received: August 18, 2014
Accepted: October 6, 2014
Published: October 6, 2014

 © 2014 American Chemical Society

small molecule and preformed polymer. There are several interesting articles in literature whereby the larger length scale phase separation afforded by block copolymers were combined with the small length scale phase separation of small molecules and mesogens to obtain higher degree of organization.[16−22] The critical challenge, however, is to replicate the success achieved independently for the donor (D) or acceptor (A) alone materials in an effective donor−acceptor combination where the wide D−A interface would afford increased charge separation and at the same time provide long-range pathway for transport of the generated charges to the respective electrodes. The increasing numbers of research articles along this direction is proof to the fact that this is a rich area with scope for further exploitation.[23,24]

In the present article we report the self-assembly of complementarily functionalized donor and acceptor materials based on oligo(*p*-phenylenevinylene) (OPV) and perylenebisimide (PBI), respectively. The main aims of the present work were to assemble the donor and acceptor molecules so as to increase the interface between them in the domain of 5−10 nm and then translate the self-assembly of the small molecules to that of the polymer, at the same time retaining the crystallinity of the small molecules. This challenging task required design of tailor-made donor and acceptor small molecules with built-in capabilities for spontaneous self-assembly as well as functionalities to aid in further hierarchical organization via polymerization. Toward this end the donor molecule based on oligo(*p*-phenylenevinylene) was functionalized with hydrogen bondable hydroxyl moiety at one end and polymerizable methacrylamide units at the other termini. The acceptor molecule based on perylenebisimide was functionalized with complementary pyridine units at one terminus and solubilizing branched alkyl chains at the other termini. The 1:1 donor−acceptor complex was further subjected to photopolymerization in the presence of photoinitiator. The complex formation and polymerization were followed in the bulk by FTIR and in solution using proton NMR spectroscopy. Photophysical studies involving UV−vis absorption and fluorescence emission were studied in solution as well as in thin film samples to understand the self-assembly between the donor and acceptor units in the 1:1 supramolecular complex as well as its polymer. Bulk structure analyses were conducted by wide-angle X-ray diffraction (WXRD) experiments. The thin film morphology of the 1:1 donor−acceptor complex and its supramolecular polymer was investigated using TEM imaging which showed the presence of lamellar organization of donor−acceptor nanostructures in the length scale of 5−10 nm. Systematic investigation of the effect of improved self-assembly on the photocurrent response of the materials was also undertaken. The study presented here is a viable route toward semiconducting donor−acceptor materials with crystallinity and processability affording better photoinduced charge separation.

EXPERIMENTAL SECTION

Materials. All chemicals were purchased from Aldrich and used as received. All solvents used were of analytical grade and carefully dried before use. Synthetic procedure to prepare the unsymmetrical oligo(*p*-phenylenevinylene) (OPVM-OH) and unsymmetrical N-substituted perylenebisimide (UPBI-Py) is given in the Supporting Information.

Sample Preparation. Unsymmetrical oligo(*p*-phenylenevinylene) (OPVM-OH) and unsymmetrical N-substituted perylenebisimide (UPBI-Py) were kept in vacuum oven for 2 days at 60 °C. 1:1 complex [UPBI-Py (OPVM-OH)]$_{1.0}$ was prepared from dry THF solution, where 1.0 denoted the number of PBI molecules per OPV molecule (theoretically). OPVM-OH was first dissolved in THF to which required amount of UPBI-Py was added and the solution was stirred at 60 °C for 24 h. The solvent was slowly evaporated on a Petri dish placed on a hot plate at 60 °C and dried further in vacuum oven at 65 °C for 2 days. After 2 days, the dried complex was stored in desiccator. To get the supramolecular polymer complex [UPBI-Py poly(OPVM-OH)]$_{1.0}$, the dried [UPBI-Py (OPVM-OH)]$_{1.0}$ complex was dissolved in dry THF. 0.2 equiv of 2,2-diethoxyacetophenone as photoinitiator was added to it and the solution irradiated for 15 min using DYMAX Blue Wave 75 light source. The solvent was evaporated on a hot plate at 60 °C and washed with hexane to remove unreacted photoinitiator. Thereafter the sample was dried in vacuum oven at 65 °C for 2 days and stored in desiccator.

Instrumentation Techniques. Infrared spectra were collected for all the samples using a Bruker α-T spectrophotometer in the range 4000−400 cm^{-1}. 1:1 complex [UPBI-Py (OPVM-OH)]$_{1.0}$ and supramolecular polymer complex [UPBI-Py poly(OPVM-OH)]$_{1.0}$, were mixed with KBr to make pellets. ^{1}H and ^{13}C NMR spectra were recorded in $CDCl_3$ using Bruker AVAENS 400 MHz spectrophotometer. Chemical shifts (δ) are reported in ppm at 298 K, with trace amount of tetramethylsilane (TMS) as internal standard. MALDI-TOF analysis was carried out on a Voyager-De-STRMALDI-TOF (Applied Biosystems, Framingham, MA, USA) instrument equipped with 337 nm pulsed nitrogen laser used for desorption and ionization. The data was collected in reflector mode with an accelerating voltage of 25 kV. Micromolar solutions of the compound in THF was mixed with 2,5-dihydroxybenzene (DHB) matrix and spotted on stainless steel MALDI plate and dried well. HRMS (ESI) were recorded on ORBITRAP mass analyzer (Thermo Scientific, Q Exactive). Mass spectra were measured with ESI ionization in MSQ LCMS mass spectrometer. Elemental analysis was done by Thermofinnigan flash EA 1112 series CHNS analyzer. Gel permeation chromatography (GPC) of all samples were performed using Viscotek VE 1122 pump, Viscotek VE 3580 RI detector and Viscotek VE 3210 UV/vis detector in tetrahydrofuran (THF) as a solvent, using polystyrene as standards. Wide angle X-ray diffraction (WXRD) was obtained using a Rigaku, MicroMax-007HF with high intensity Microfocus rotating anode X-ray generator. All the samples were recorded in the (2θ) range 3−50° and data was collected with the help of Control Win software. A Rigaku, R-axis IV^{+2} detector was employed in wide-angle experiments. The radiation used was Cu Kα (1.54 Å) with a Ni filter, and the data collection was carried out using an aluminum holder. Small angle X-ray scattering (SAXS) was employed to investigate the phase behavior of the complexes. The scattering experiments were conducted on a three pinhole collimated Bruker Nanostar machine equipped with rotating copper anode, operating at 45 kV and 100 mA providing characteristic Kα radiation of 1.54 Å. The measurements were carried out in the normal resolution mode having a q range 0.011−0.2 Å^{-1}. The bulk sample was taken in between two Kaptan film. The scattered data was collected using a 2-D Histar detector and later converted from 2D to 1D by azimuthal averaging using Bruker software. 1D data presented after background subtraction is plotted as I v/s q, where q = ($4\pi/\lambda$) Sinθ, λ is the wavelength of the incident X-rays and 2θ is the scattering angle. Transmission Electron microscopy (TEM) was done using an FEI-Tecnai-F20 electron microscope operating at 200 kV. The photo polymerization was performed with DYMAX Blue Wave 75 W short arc mercury vapor lamp as light source with an output wavelength in the range 280−450 nm. A PerkinElmer Lambda 35 UV spectrophotometer was used for measuring absorption spectrum. Steady-state fluorescence studies and time-resolved fluorescence lifetime measurements were conducted on a Horiba Jobin Yvon Fluorolog 3 spectrophotometer having a 450 W xenon lamp. The steady-state fluorescence studies were carried out in DMF, ODCB as well as in thin film drop casted from DMF. Throughout the experiments, emission and excitation slit width was maintained at 1 nm, and the data were obtained in "S1/R1" mode. The fluorescence lifetime studies were carried out for samples drop cast as films from DMF. Nano LED of 370 nm was used for fluorescence lifetime measurements and data was collected at 450 nm (OPV) and 625 nm (PBI). The decay curves were obtained by the time correlated single photon counting (TCSPC)

Scheme 1. Synthesis of Hydroxyl Functionalized Oligo(*p*-phenylene vinylene) Methacrylamide (OPVM-OH)

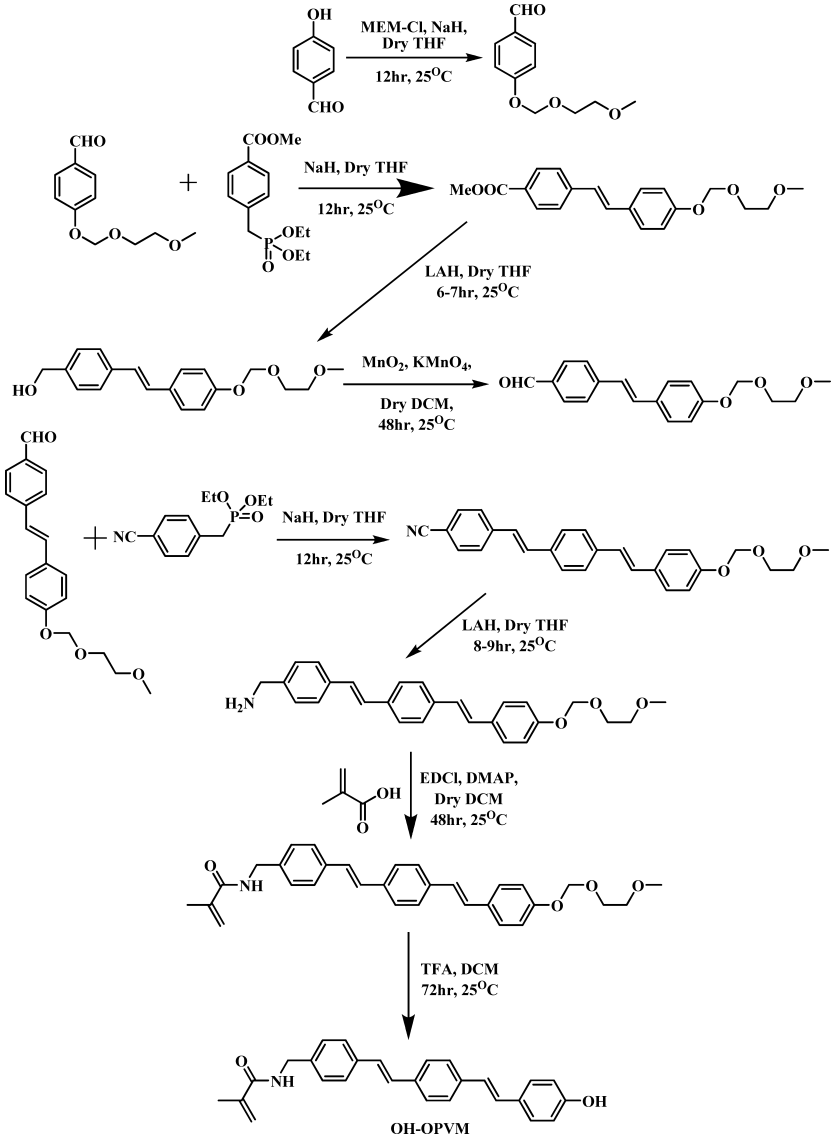

Scheme 2. Synthesis of Unsymmetrical Perylene Bisimide UPBI-Py

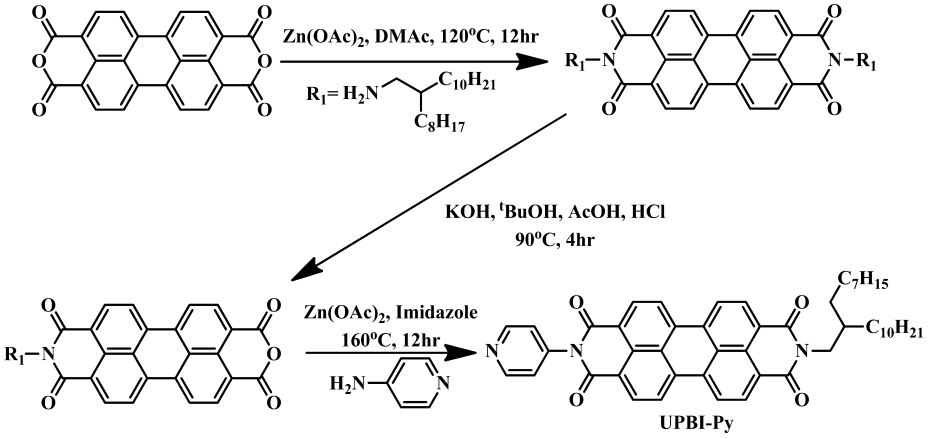

technique. Fluorescence lifetime values were determined by deconvoluting the data with exponential decay using DAS6 decay analysis software. The quality of fit was judged by fitting parameters such as $\chi^2 \approx 1$, as well as the visual inspection of the residuals and autocorrelations.

SCLC Device Fabrication. SCLC mobility and AC photocurrent measurements were performed on ITO/polymer (complex)/Al sandwiched structures. Polymer/complex solution was drop casted from ODCB (Ortho dichlorobenzene) on cleaned ITO (sheet resistance 15Ωsq^{-1}). Aluminum top contacts with thickness of 80

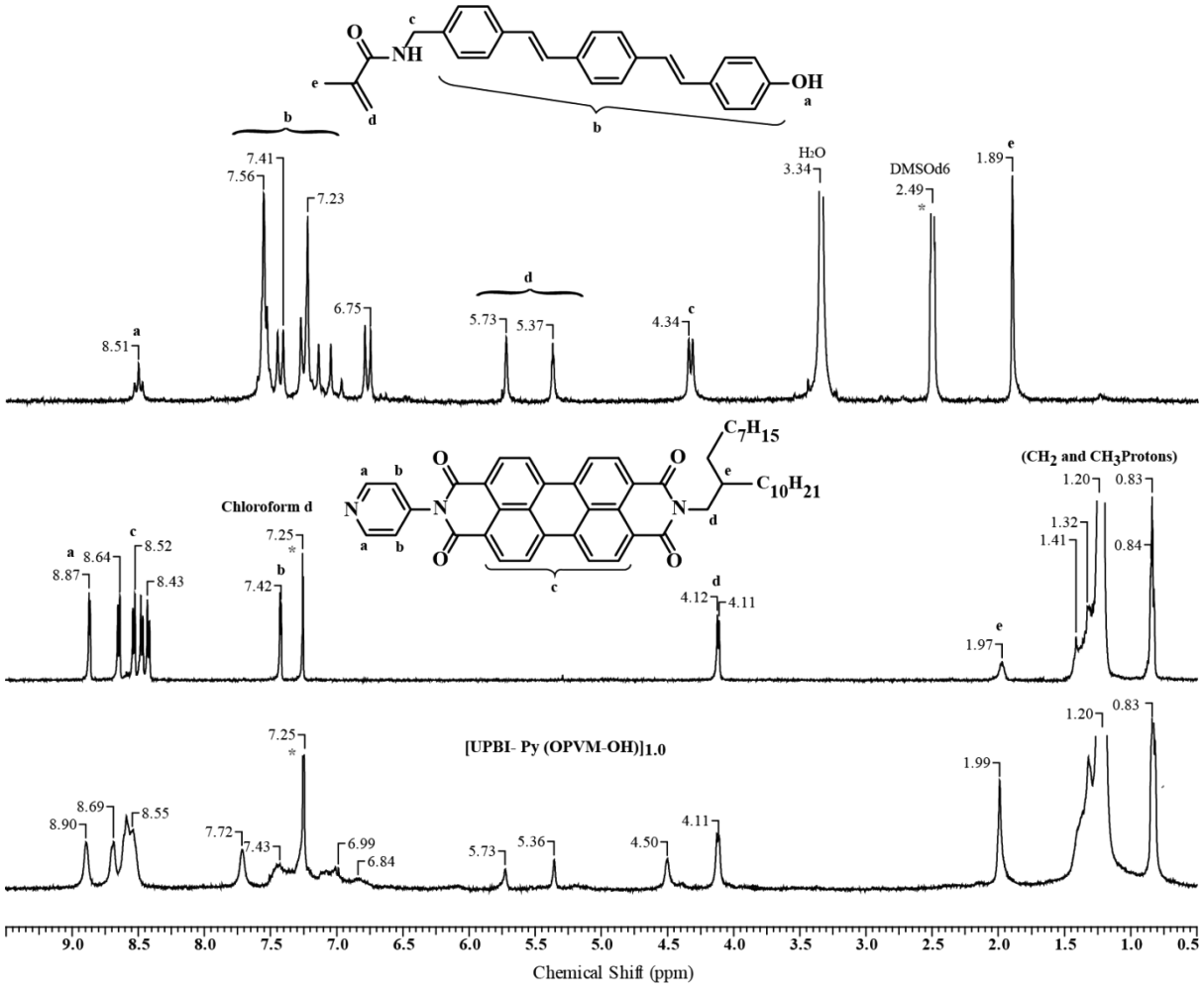

Figure 1. Comparison of the ^{1}H NMR spectra of OPVM-OH (recorded in DMSO-d_6), UPBI-Py and the 1:1 complex $[\text{UPBI-Py (OPVM-OH)}]_{1.0}$ recorded in $CDCl_3$ at 25 °C.

Scheme 3. Structure of Complex $[\text{UPBI-Py (OPVM-OH)}]_{1.0}$ Formed by the Unsymmetrical UPBI-Py with OPVM-OH

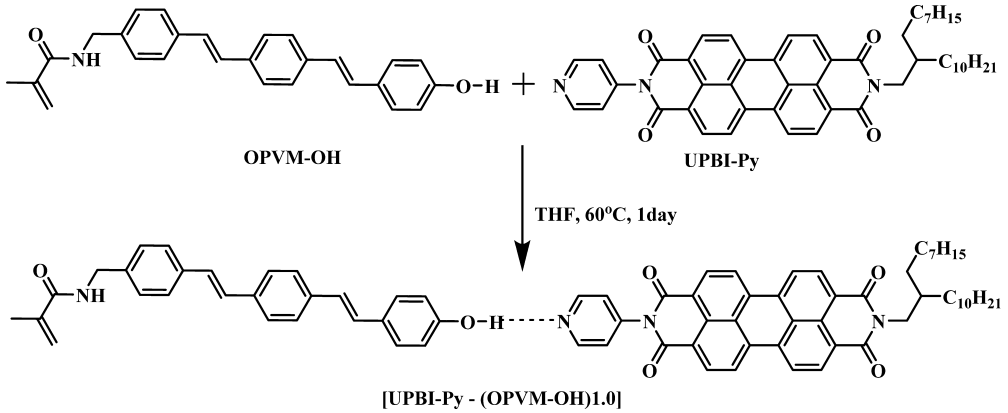

nm and area ~6 × 10^{-2} cm^2 were thermally evaporated on to the polymer through shadow mask, at the rate of 1 Å/s and under pressure of 5 × 10^{-6} mbar. Thickness of the polymer coatings (1−4 μm) were measured using Dektak surface profiler. SCLC and photocurrent measurements were carried out while keeping device in vacuum (10^{-3} mbar). Incident light from Tungsten −halogen source was modulated at 20 Hz and the photocurrent was measured using a lock-in Amplifier (Stanford SR830). The data was normalized to incident photon density using a commercial calibrated photodiode under similar experimental conditions.

RESULTS AND DISCUSSION

Synthesis and Characterization. The donor molecule OPVM-OH based on oligo(*p*-phenylenevinylene) (OPV) was synthesized as shown in Scheme 1 with polymerizable methacrylamide groups at one end and hydrogen bondable hydroxyl unit at the other termini. The acceptor molecule UPBI-Py based on unsymmetrical N-substituted perylenebisimide (PBI) was synthesized in reasonable yield and purity following the procedure shown in Scheme 2. The details of the

Scheme 4. Photo Polymerization of the 1:1 Complex $[\text{UPBI-Py (OPVM-OH)}]_{1.0}$ to Yield $[\text{UPBI-Py Poly(OPVM-OH)}]_{1.0}$

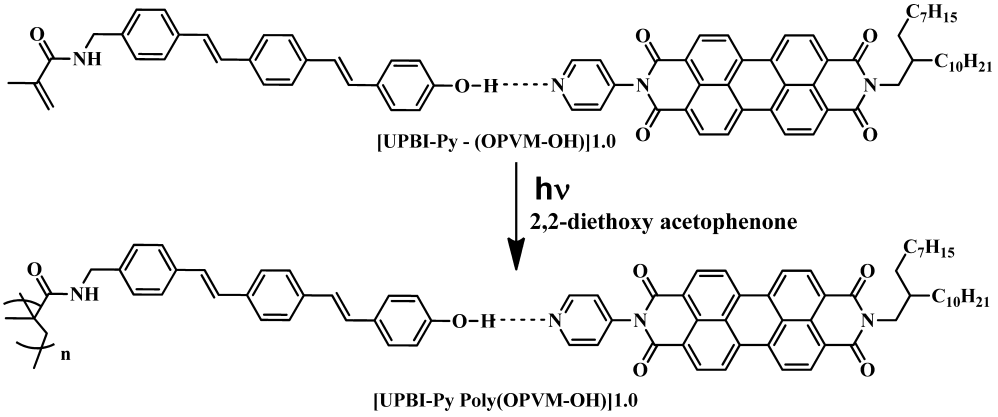

synthesis are given in the Supporting Information (SI) . The donor and acceptor molecules were subjected to repeated column chromatographic purification to obtain the final molecules in extremely pure form. The structure was confirmed by proton NMR (Figure 1), MALDI-TOF (SI Figure S1 (a-b)) and FTIR (SI Figure S2) measurements and purity confirmed by HRMS/elemental analysis and size exclusion chromatogram (SEC) (SI Figure S3). Figure 1 shows the labeled proton NMR spectra of the OPV and PBI molecules. Due to poor solubility in chloroform, the ^{1}H NMR spectra of OPVM-OH was recorded in dimethyl sulfoxide (DMSO-d_6). The OPV aromatic protons as well as vinylic protons appeared in the range 7.56–6.75 ppm and the methacrylic protons appeared as two singlets at 5.73 and 5.37 ppm. In the proton NMR spectra of UPBI-Py, the eight aromatic protons of perylene core appeared as four doublets in the region 8.64–8.43 ppm, while the aromatic protons of the pyridine ring appeared as doublets at 8.87 and 7.42 ppm.

The supramolecular assembly of n-type organic semiconductor perylenebisimide (PBI) with p-type organic semiconductor oligo(*p*-phenylenevinylene) (OPV), involving noncovalent secondary interactions such as hydrogen-bonding and $\pi-\pi$ stacking interactions were investigated. The complex was prepared by dissolving 1:1 molar ratio of UPBI-Py and OPVM-OH in dry tetrahydrofuran (THF) as solvent, stirring at 60 °C for 24 h, followed by removal of solvent by heating (Scheme 3). The complex was named $[\text{UPBI-Py (OPVM-OH)}]_{1.0}$, where 1.0 denoted the theoretical 1:1 ratio of UPBI-Py and OPVM-OH. Successful complex formation was indicated by the improved solubility of the complex compared to the respective pure components. Detailed structural characterization of the complex was carried out using proton NMR spectroscopy in deuterated chloroform, in which the complex was now soluble, in contrast to the poor solubility of OPVM-OH. The amino pyridine aromatic ring protons at 8.87 ($H_{\alpha\text{-Py}}$) and 7.42 ($H_{\beta\text{-Py}}$) ppm in UPBI-Py[25] shifted downfield to 8.90 and 7.72 ppm respectively upon complex formation. The downfield shift of the inner pyridine protons from 7.42 to 7.72 ppm was rather surprising. A two-dimensional correlation spectroscopy (COSY) experiment on $[\text{UPBI-Py (OPVM-OH)}]_{1.0}$ in $CDCl_3$+DMSO-d_6 showed a cross coupling of the two peaks at 7.72 and 8.90 ppm confirming that they were indeed the aromatic protons of the pyridine ring of UPBI-Py. An overall broadening of all the peaks was also surprisingly observed in the complex.

The formation of the complex was traced by FTIR spectroscopy also. The pyridine ring in UPBI-Py has a symmetric ring stretching vibration at 1093 cm^{-1}. In general, the nitrogen atom in pyridine derivatives such as 4-vinylpyridine has a pyridine breathing mode ~996 cm^{-1}.[26] The absorption at 1093 cm^{-1} in UPBI-Py was assigned to the pyridine ring stretching vibration based on comparison with a symmetric perylenebisimide molecule having only alkyl substitution on both termini, which lacked the absorption at 1093 cm^{-1} (SI Figure S2-a). After complexation, a shift to higher wavenumber (1105 cm^{-1}) was observed upon hydrogen bonding interaction with the phenol unit of OPVM-OH (SI Figure S2-b). Other characteristic pyridine C═N symmetric stretching vibration at 1271 and 1511 cm^{-1} were difficult to trace due to considerable overlap from other OPV stretching vibrations. Hydrogen bonding interaction of the >C═O group in the amide linkage in OPVM-OH was ruled out as this stretching vibration at 1656 cm^{-1} (SI Figure S2-c) remained unchanged upon complex formation clearly indicating its lack of participation in any noncovalent interaction.

Polymerization. The photoinduced polymerization of the 1:1 OPV-PBI complex was carried out in the presence of photoinitiator 2,2-diethoxyacetophenone. A dry THF solution of the complex (10 mg in 3 mL) with 0.2 equiv of photoinitiator was irradiated for 15 min using a DYMAX Blue Wave 75 light source (Scheme 4). Afterward, the solvent was removed; the residue washed with hexane to remove the photoinitiator and then the sample was analyzed using FTIR as well as proton NMR spectroscopic techniques. The same photopolymerization experiment was repeated under identical conditions for the OPV molecule OPVM-OH also. Upon evaporation of the solvent THF at the end of 15 min of irradiation, followed by hexane washing, a film of the homopolymer poly(OPVM-OH) was obtained. This homo polymer of OPV was completely insoluble in common organic solvents such as chloroform, dimethylformamide (DMF) and THF. Hence structural characterization using proton NMR spectroscopy was unfortunately not possible. However, the FTIR spectra was recorded of the solid homopolymer sample and compared with that of the supramolecular polymer complex. The supramolecular polymer complex was represented as $[\text{UPBI-Py poly(OPVM-OH)}]_{1.0}$ in the manuscript to indicate that the polymerization occurred on the OPVM-OH moiety. The disappearance of the characteristic methacrylate double bond at 836 cm^{-1} was followed using FTIR spectra.[27,28] SI Figure S2-d compares the expanded normalized FTIR

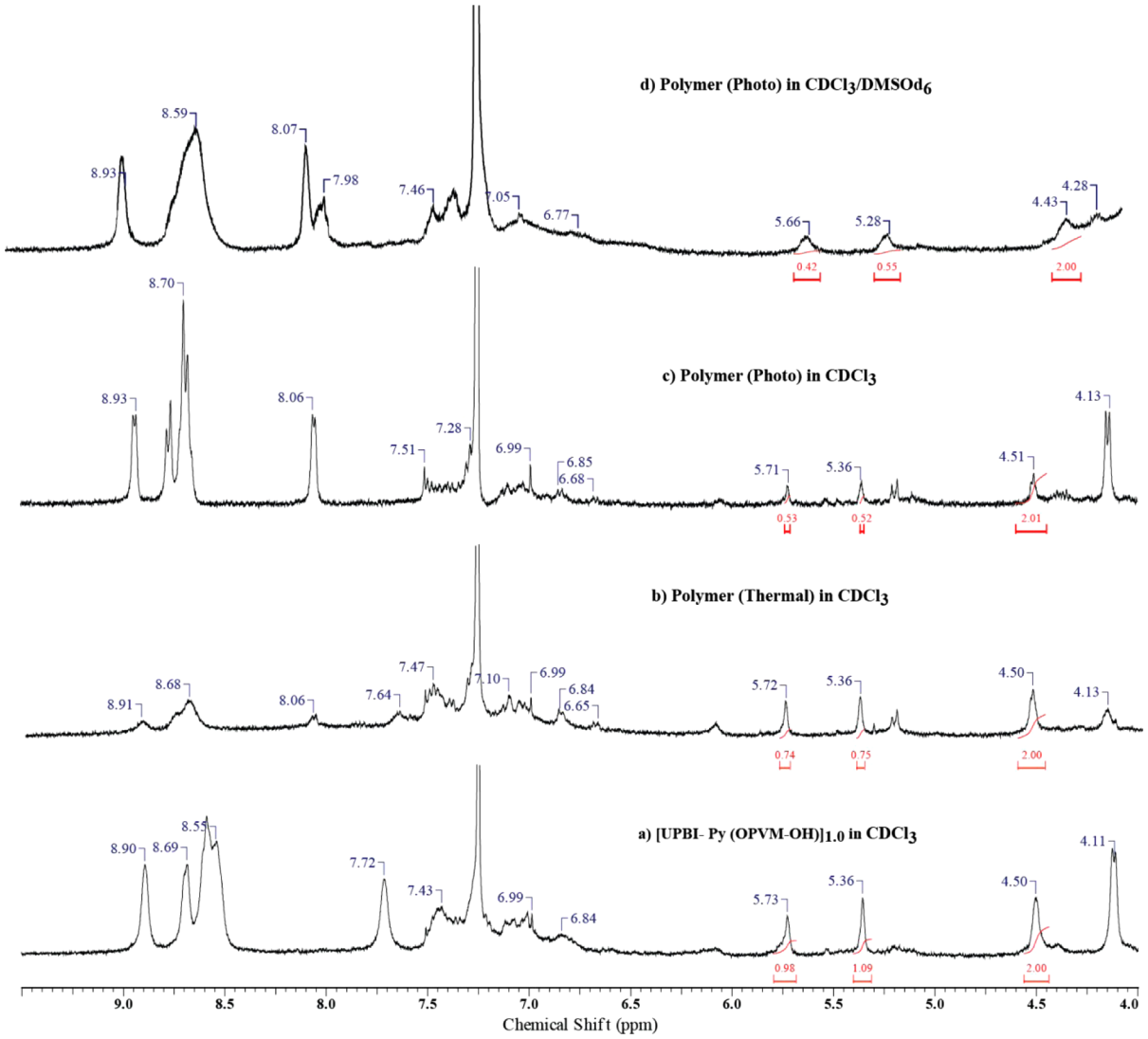

Figure 2. Comparison of the ^{1}H NMR spectra of $[UPBI\text{-}Py\ (OPVM\text{-}OH)]_{1.0}$ with the supramolecular polymer $[UPBI\text{-}Py\ poly(OPVM\text{-}OH)]_{1.0}$ prepared thermally as well as by photopolymerization recorded at 25 °C in $CDCl_3$ as well as in mixture of $CDCl_3$/DMSO-d_6.

spectra of solid samples of the complex before and after photopolymerization along with that of OPVM-OH. The spectra were normalized at 965 cm^{-1} corresponding to OPV vibrations, where UPBI-Py did not have any absorbance. The peak at 836 cm^{-1} was clearly observable in the 1:1 complex $[UPBI\text{-}Py\ (OPVM\text{-}OH)]_{1.0}$ but was reduced in intensity in the supramolecular polymer complex $[UPBI\text{-}Py\ poly(OPVM\text{-}OH)]_{1.0}$. In the polymer, a broad peak at 812 cm^{-1} corresponding to UPBI-Py was observed. It was difficult to trace the extent of polymerization from the FTIR spectra due to the close overlap of other peaks.

An attempt was made to characterize the supramolecular complex and polymer using gel permeation chromatography (GPC). The SI Figure S3-a compares the gel permeation chromatograms of the $[UPBI\text{-}Py\ (OPVM\text{-}OH)]_{1.0}$ and $[UPBI\text{-}Py\ poly(OPVM\text{-}OH)]_{1.0}$ along with that of UPBI-Py and OPVM-OH recorded in THF − a solvent in which all the samples were soluble. The difference in molar mass between UPBI-Py and OPVM-OH was not so large so that their chromatograms overlapped to a large extent with very narrow time difference in their elution. The SEC chromatograms of $[UPBI\text{-}Py\ (OPVM\text{-}OH)]_{1.0}$ and $[UPBI\text{-}Py\ poly(OPVM\text{-}OH)]_{1.0}$ were broader and appeared in between that of the starting components. GPC is expected to differentiate a mixture of two different compounds provided they differ considerably in their masses. The narrow difference in mass of the two components involved in the supramolecular complex formation made their molecular weight characterization by GPC not reliable. In fact, a 1:1 molar mixture of UPBI-Py and OPVM-OH was prepared by mixing the powdered solid samples together. A solution of this sample was then prepared for GPC analysis in THF and injected into the GPC column. A part of the solid mixture was dissolved in THF and subjected to photopolymerization under conditions identical to that described earlier. This sample named as phymix polymer was also analyzed for its molecular weight by injecting into the GPC column. SI Figure S3-b compares the GPC chromatograms of the 1:1 physical mixture of UPBI-Py + OPVM-OH and phymix polymer sample. The GPC chromatograms appeared in between that of UPBI-Py and OPVM-OH. Even the 1:1 UPBI-Py + OPVM-OH did not appear as two separate peaks or as a peak with a shoulder demonstrating that the mass difference between UPBI-Py and OPVM-OH was not large enough for the GPC to differentiate among them. However, it

dx.doi.org/10.1021/am5055542 | ACS Appl. Mater. Interfaces 2014, 6, 19434−19448

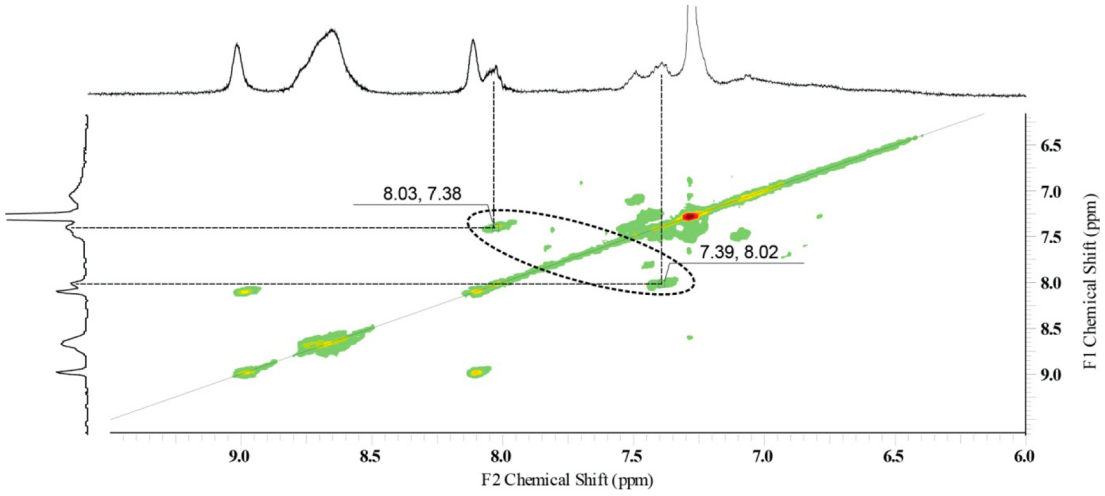

Figure 3. COSY spectra of $[\text{UPBI-Py poly(OPVM-OH)}]_{1.0}$ showing selected NOE extract of the aromatic region (400 MHz, $CDCl_3$/DMSO-d_6, 298 K). The peaks showing diagonal cross coupling is encircled.

should also be mentioned here that besides the lack of sensitivity of our GPC instrument to differentiate between the two low molecular weight samples, GPC would not be a good choice for characterizing self-assembly in very dilute samples. Self-assembly being a dynamic process, complexation is not favored under very dilute conditions. Noticeable from the GPC data was the shift in the chromatogram of the supramolecular polymer to higher molecular weight compared to that of OPVM-OH clearly demonstrating that at least oligomers were formed.

The ^{1}H NMR spectra of the supramolecular polymer complex $[\text{UPBI-Py poly(OPVM-OH)}]_{1.0}$ was recorded in $CDCl_3$ and compared with that of the complex as shown in Figure 2a,c (expanded region from 4.0 to 9.5 ppm). The proton NMR spectra showed the presence of unreacted methacrylate double bond in the polymer, but its intensity had reduced compared to the OPV aromatic protons. The extent of double bond conversion was estimated from the proton NMR integration values of the methacrylic peaks with respect to the peak at 4.5 ppm corresponding to two protons next to the amide linkage in OPVM-OH. The extent of polymerization was calculated to be around 48%. Free radical polymerization using BPO as the initiator and THF as solvent was also carried out to see if higher conversion could be achieved thermally. Figure 2b shows the proton NMR spectra of the supramolecular polymer complex synthesized thermally. The proton NMR spectra of the polymers covering the full chemical shift range are given in the SI Figure S4. The extent of thermal polymerization was calculated to be ∼30%. Another noticeable observation from the comparison of the proton NMR spectra of the complex and the polymer was the further downfield shift of the $H_{\beta\text{-Py}}$ of UPBI-Py from 7.72 to 8.06 ppm upon polymerization. This shift was observed for both the thermally polymerized sample as well as photopolymerized sample ruling out any photodegradation of the sample as the reason for this downfield shift by 0.34 ppm. Compared to the pristine UPBI-Py, the overall shift upon polymerization after complex formation was ∼0.64 ppm, which was quite surprising considering the fact that the point of polymerization was on the OPV, which was spatially farther apart from UPBI-Py. Figure 2d also shows the proton NMR spectra of the polymer recorded in a mixture of solvents, namely, $CDCl_3$/DMSO-d_6. Addition of a few drops of DMSO-d_6 improved the solubility of the polymer considerably allowing higher concentration to be maintained. COSY experiments were conducted on the supramolecular polymer complex (in the solvent mixture $CDCl_3$/DMSO-d_6) to identify through-space couplings within the sample. Figure 3 shows the COSY spectra highlighting the aromatic region of the $[\text{UPBI-Py poly(OPVM-OH)}]_{1.0}$. In addition to the cross coupling of the two peaks at 7.72 and 8.90 ppm corresponding to the $H_{\alpha\text{-Py}}$ and $H_{\beta\text{-Py}}$ protons of the pyridine ring of UPBI-Py, which was observed for the 1:1 complex, new off-diagonal peaks were observed connecting resonances from UPBI-Py and OPVM-OH. This is shown encircled in Figure 3 indicating that the $H_{\beta\text{-Py}}$ protons of the pyridine ring of UPBI-Py at 8.02 ppm was spatially close to the aromatic protons of OPVM-OH at 7.30 ppm. This could explain the large downfield shift of 0.64 ppm observed for the $H_{\beta\text{-Py}}$ protons of the pyridine ring of UPBI-Py upon polymerization followed by complexation with OPVM-OH.

Photophysical Characterization. Photophysical studies involving UV−visible absorption and fluorescence spectroscopy measurements were undertaken to get more insight into the nature of self-assembly of the donor−acceptor complex formed by UPBI-Py and OPVM-OH. DMF was used as the solvent for the photophysical studies since OPVM-OH had better solubility in DMF. Figure 4a shows the normalized absorption spectra of UPBI-Py and OPVM-OH taken in solution in DMF as well as drop cast as thin films from DMF. In solution, the absorption spectra of OPVM-OH was characterized by a broad spectra with peak at 375 nm, while UPBI-Py exhibited characteristic absorption of isolated perylene bisimide chromophore with peaks in the range 400−530 nm. The absorption spectrum in the solid state had more vibrational fine structures and the absorption maximum was blue-shifted from 375 in solution to ∼325 nm in film for OPVM-OH indicating H type aggregation.[29] In the case of films of UPBI-Py, the absorption was broad, and the peak intensities of the $A^{0\rightarrow0}$ and $A^{0\rightarrow1}$ changed compared with that of the solution spectrum. The ratio of the peak intensities of absorbance $A^{0\rightarrow0}/A^{0\rightarrow1}$ lower than 1.6 is generally taken as an indication for aggregation.[30−32] The value of this ratio in the film was 1.03, suggesting aggregation in the solid state. The peak maxima blue-shifted and a new red-shifted peak appeared at 547 nm, which were features attributed to rotationally shifted face-to-face aggregates.[32]

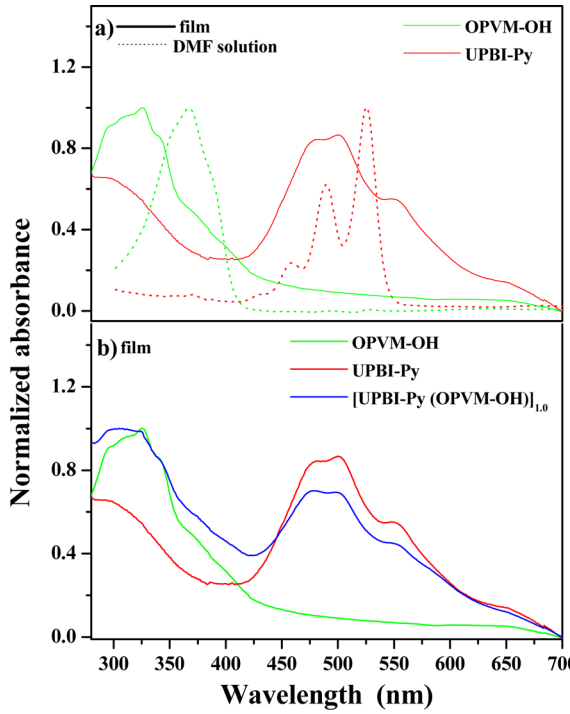

Figure 4. (a) Absorption spectrum of OPVM-OH and UPBI-Py in DMF solution and dropcasted (from DMF) film. (b) Comparison of absorption spectrum of drop cast film of $[UPBI\text{-}Py\ (OPVM\text{-}OH)]_{1.0}$ along with that of OPVM-OH and UPBI-Py.

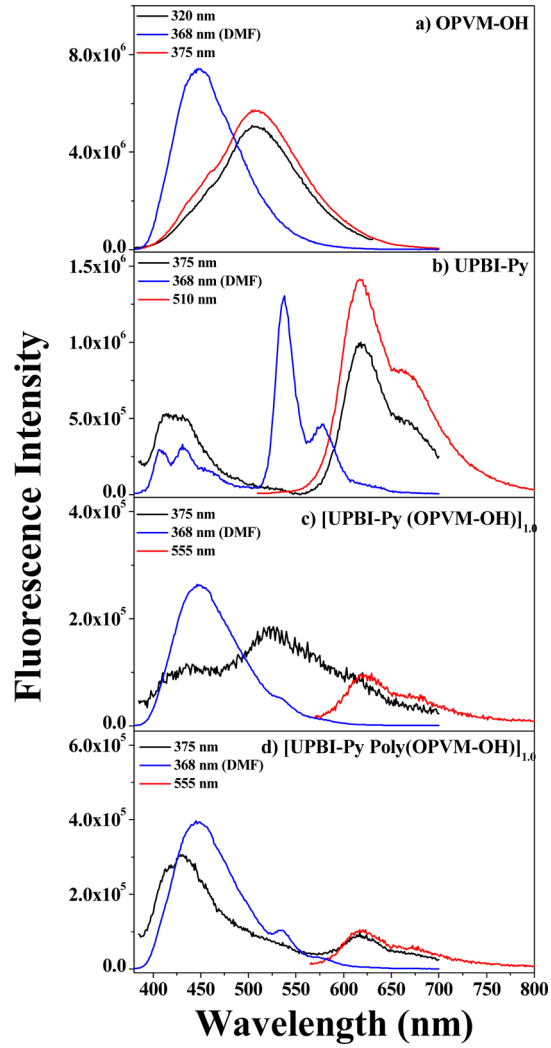

Figure 5. Fluorescence spectrum of (a) OPVM-OH, (b) UPBI-Py, (c) $[UPBI\text{-}Py\ (OPVM\text{-}OH)]_{1.0}$, and (d) $[UPBI\text{-}Py\ poly(OPVM\text{-}OH)]_{1.0}$ upon excitation at different wavelengths in DMF solution (blue line) and as drop cast films from DMF.

The normalized absorption spectra of drop cast films (from DMF) of the 1:1 complex $[UPBI\text{-}Py\ (OPVM\text{-}OH)]_{1.0}$ exhibited features corresponding to both the OPV and PBI chromophores. The normalized absorption spectra comparing the features of OPVM-OH, UPBI-Py, and $[UPBI\text{-}Py\ (OPVM\text{-}OH)]_{1.0}$ are given in Figure 4b, while the absorption spectra plotted as a function of molar extinction coefficient (to highlight the contribution of each chromophore) is given in SI Figure S5a. No charge transfer band was observed in the absorption spectra of films of the DA complex indicating the absence of electronic communication between donor and acceptor moieties in the ground state.[33] The OPV absorption in the range 280 to 400 nm was more broadened due to the overlapping absorption of PBI also occurring in the same range. It was clear that both the OPV and PBI chromophores were aggregated in the 1:1 complex also since they were blue-shifted and exhibited features similar to that of the aggregated starting materials.

Figure 5 compares the emission spectra of OPVM-OH, UPBI-Py, $[UPBI\text{-}Py\ (OPVM\text{-}OH)]_{1.0}$, and $[UPBI\text{-}Py\ poly\text{-}(OPVM\text{-}OH)]_{1.0}$ upon excitation at both the OPV (368 nm in DMF solution and 375 nm in film) and PBI (~555 nm) emission wavelengths as drop cast films from DMF. The figure also includes the emission spectra recorded in DMF solution (blue line) for all samples upon excitation at the OPV absorption maximum of 368 nm. OPVM-OH exhibited strong emission with maximum at 445 nm in DMF solution (Figure 5a). In the solid state upon excitation at 375 nm, the OPV monomer emission at 445 nm was suppressed and a broad red-shifted aggregate emission was observed with peak at 500 nm. The blue-shifted absorption together with the red-shifted emission in film compared to that in solution has been shown to be due to existence of H type aggregates in film.[34] Upon excitation at the OPV wavelength ~375 nm, UPBI-Py exhibited intense emission (both DMF solution as well as film), which indicated that selective excitation of the OPV chromophore was not feasible. Two small peaks were observed at 410 and 430 nm along with typical emission of perylene bisimides with peak maxima at 534, 576, 626 nm in DMF (Figure 5b). However, in the solid state the PBI monomer emission at 534 nm was hugely suppressed, and a red-shifted intense broad emission was observed at 638 nm indicating aggregate formation. Upon excitation at 510 nm corresponding to PBI absorption wavelength maximum, the emission peak shape remained the same showing aggregate emission at 638 nm, but the intensity was slightly higher.

Figure 5c compares the emission from the 1:1 supramolecular donor−acceptor complex $[UPBI\text{-}Py\ (OPVM\text{-}OH)]_{1.0}$ upon excitation around 370 nm both in DMF solution and as films. The emission from the film was considerably quenched compared to that in solution; therefore, the emission spectra collected in DMF had to be scaled down by a factor of 30 to plot them together. The emission from the D−A complex in DMF solution was very similar to that of the emission from molecularly dissolved OPVM-OH collected in DMF with

dx.doi.org/10.1021/am5055542 | ACS Appl. Mater. Interfaces 2014, 6, 19434−19448

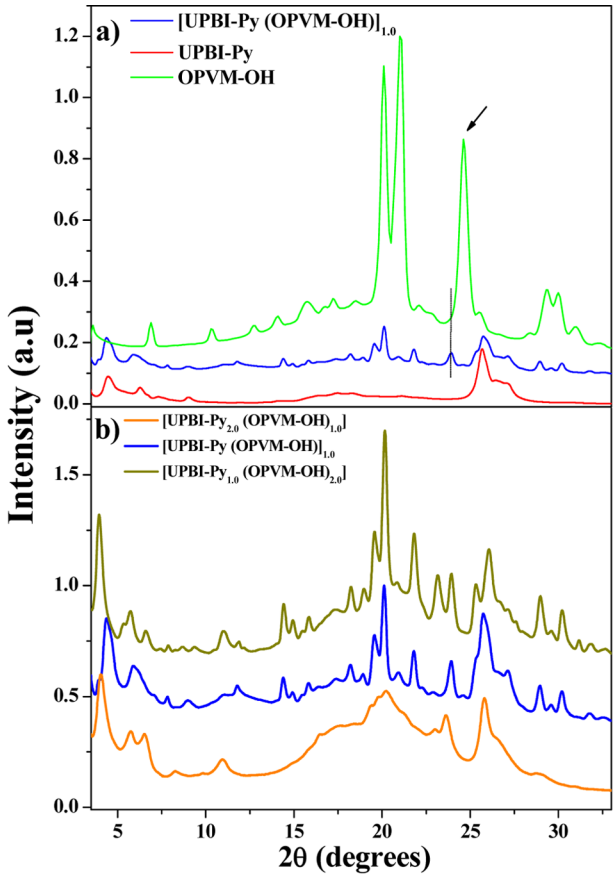

(c)

Sample Name	a (Å)	b (Å)	c (Å)	β	V
OPVM-OH	29.843(24)	3.613(3)	25.709(23)	122.74(5)	2331.71
[UPBI-Py$_{1.0}$ (OPVM-OH)$_{2.0}$]	31.675(19)	4.920(3)	17.326(20)	104.37(8)	2616.06
[UPBI-Py (OPVM-OH)]$_{1.0}$	34.774(21)	4.537(3)	16.97(10)	118.13(5)	2363.51
[UPBI-Py$_{2.0}$ (OPVM-OH)$_{1.0}$]	33.07(16)	4.387(4)	16.214(18)	98.68(19)	2325.59

Figure 6. Wide angle X-ray diffraction pattern recorded at 25 °C (2θ from 2 to 35°) for (a) OPVM-OH, UPBI-Py, and 1:1 complex [UPBI-Py (OPVM-OH)]$_{1.0}$; (b) the three complexes [UPBI-Py (OPVM-OH)]$_{1.0}$, [UPBI-Py$_{1.0}$ (OPVM-OH)$_{2.0}$] and [UPBI-Py$_{2.0}$ (OPVM-OH)$_{1.0}$]; (c) table giving the unit cell parameters.

maximum at 445 nm. However, a small shoulder was observed around 550 nm corresponding to emission from molecularly dissolved UPBI-Py. Although selective excitation of OPV was not possible and PBI chromophore also could be excited by excitation at 368 nm, a part of the PBI emission upon excitation at 368 nm could have contribution from energy transfer occurring from OPV to PBI also. This was supported by the observation of OPV absorption band in the excitation spectra of [UPBI-Py (OPVM-OH)]$_{1.0}$ collected while monitoring the PBI emission at 540 nm (SI Figure S5b). Upon excitation at 375 nm, the emission from films of [UPBI-Py (OPVM-OH)]$_{1.0}$ exhibited broad emission centered at 525 nm with shoulder at 430 and 620 nm. The emission of OPV at 525 nm was quenched 36 times in [UPBI-Py (OPVM-OH)]$_{1.0}$ compared to that in the OPVM-OH alone. This was an indication of energy transfer from OPVM-OH to UPBI-Py in the film state in the 1:1 supramolecular complex. Unambiguous identification of the nature of origin of the peak around 420 nm was not easy since PBI as well as unaggregated OPV had emission in the same region. However, the shoulder at 630 nm could be attributed to the aggregate emission occurring from PBI units as could be confirmed from the emission spectra collected by exciting at 555 nm corresponding to PBI.

An attempt was made to obtain evidence for energy transfer from OPVM-OH to UPBI-Py in [UPBI-Py (OPVM-OH)]$_{1.0}$ from the fluorescence emission lifetime decay studies. The

sample films were excited using a nanoLED source of 370 nm and monitored at the OPV emission of 450 nm as well PBI emission of 625 nm. Although the best fits were obtained to be biexponential, the most prominent species (α_1 = 0.99) in OPVM-OH film had a lifetime of 0.42 ns (table in SI Figure S5c). This was much lower compared to the fluorescence emission decay value of 1.01 ns observed for OPVM-OH in solution (DMF).[35] The reduced lifetime for the emitting species confirmed quenching due to aggregation in the solid state. The 1:1 supramolecular donor−acceptor complex [UPBI-Py (OPVM-OH)]$_{1.0}$ was also excited at 370 nm and the decay observed both at the OPV emission region of 450 nm and PBI emission region of 625 nm. At the OPV emission region of 450 nm, an emission lifetime decay of 0.48 ns (α_1 = 0.98) was observed, while at the PBI emission region of 625 nm, a decay of 1.11 ns (α_1 = 0.98) was observed. The increase in OPV emission lifetime decay values instead of the expected decrease in the donor−acceptor complex could be understood by studying the lifetime decay profile of UPBI-Py upon excitation at 370 nm. Upon exciting UPBI-Py at the OPV absorption wavelength of 370 nm, a decay time of 0.54 ns (α_1 = 0.97) was observed, which made establishment of existence of energy transfer from OPV chromophore to PBI impossible. The observed emission from PBI (at 625 nm) upon excitation at 370 nm also could not be unambiguously attributed to energy transfer process, because UPBI-Py alone exhibited emission at 625 nm with a lifetime decay of 1.11 ns (α_1 = 0.98) for the 370 nm excitation. However, the increased extent (36 times) of the OPV fluorescence quenching at 525 nm in [UPBI-Py (OPVM-OH)]$_{1.0}$ compared to that in the OPVM-OH alone gave indirect evidence for the existence of energy transfer channels between OPV and PBI in the 1:1 supramolecular donor−acceptor complex.

The supramolecular polymeric complex [UPBI-Py poly-(OPVM-OH)]$_{1.0}$, which was obtained by photopolymerization of the [UPBI-Py (OPVM-OH)]$_{1.0}$ complex, was also subjected to photophysical characterization. SI Figure S5d shows the absorption spectra of thin film sample of the polymer along with that of the 1:1 complex. Figure 5d shows, the emission in DMF solution (excitation: 368 nm; scaled down by a factor of 15) was very similar to that of [UPBI-Py (OPVM-OH)]$_{1.0}$ with OPV emission peak at 445 nm having a shoulder peak at 550 nm corresponding to emission from molecularly dissolved perylene bisimide. The emission spectrum of thin film samples of the polymer was different from that of thin films of the 1:1 supramolecular complex. The monomeric OPV emission was observed with an almost complete suppression of the OPV aggregate emission beyond 500 nm in the polymer film. The emission was characterized by two peaks in its emission spectra, one at 429 nm with a shoulder at 417 nm and another peak at 618 nm corresponding to aggregated PBI emission. Although PBI also exhibited emission around 420 nm, based on the higher intensity of emission with respect to the PBI aggregate emission at 618 nm the peaks at 429 nm could be attributed to nonaggregated OPV emission. The OPV monomeric emission at 429 nm was very similar to that of OPVM-OH in dilute solution with peak at 430 nm. The emission spectra of the insoluble homopolymer poly(OPVM-OH) (produced by the photopolymerization of OPVM-OH) was recorded as solid powder sample and compared with that of the supramolecular polymer complex. SI Figure S5e compares the emission from thin film sample of [UPBI-Py poly(OPVM-OH)]$_{1.0}$, along with that of the emission from powder sample of poly(OPVM-OH). The homopolymer poly(OPVM-OH) was characterized by two peaks in the emission spectra—one at 503 nm identical with that of thin film of its monomer OPVM-OH and another new red-shifted peak at 570 nm. The new red-shifted peak could have its origin in excimer luminescence originating from polymer interchain excitations.[35,36] It is interesting to analyze the emission characteristics of the supramolecular donor−acceptor polymer in the context of the behavior of the donor homopolymer. Although the starting donor−acceptor supramolecular complex exhibited red-shifted aggregate emission of OPV, this aggregate was disrupted upon polymerization. It was evident that the donor−acceptor small molecule assembly upon polymerization of the donor units exhibited a drastic change in emission characteristics of the donor, reflecting the change in organization of the donor units brought about by covalent linkage of their methacrylamide backbone.

In order to rule out the role of the solvent (DMF) used for preparing the sample films influencing their self-organization, the 1:1 supramolecular donor−acceptor complex and its polymer films were prepared from another solvent−ortho dichlorobenzene (ODCB)—a solvent from which devices were prepared for bulk mobility estimate (described later). SI Figure S5f compares the emission at 375 nm from the sample films of 1:1 supramolecular donor−acceptor complex and its polymer prepared from both DMF and ODCB. The emission characteristics were similar in both sets of films suggesting that the changes observed in the emission spectra of the polymer was not brought about by solvent effect, but it had its origin in the changes in organization of the donor occurring due to polymerization. Thus, the photophysical studies involving emission from thin film samples established the donor−acceptor assembly in the 1:1 supramolecular complex as well as provided evidence for subtle changes occurring in their self-assembly upon covalent linkage of the methacrylamide units into a polymeric backbone in the donor moieties.

Bulk Structure Analysis. Figure 6a shows the normalized WXRD patterns for UPBI-Py, OPVM-OH, and the 1:1 complex [UPBI-Py (OPVM-OH)]$_{1.0}$ measured at room temperature (25 °C) in the range 2θ = 2.5−35°. OPVM-OH did not exhibit any peak below 2θ = 3°, which was independently confirmed by small-angle X-ray scattering (SAXS) analysis (given in SI Figure S6). Compared to UPBI-Py, OPVM-OH was more crystalline with several sharp peaks covering the entire 2θ range from 2.5 to 35°. Attempts to index UPBI-Py were not successful; however, most of the peaks in the pattern of OPVM-OH could be successfully indexed and fitted to a monoclinic crystal lattice with cell parameters a = 29.843(24), b = 3.613(3), c = 25.709(23), and β = 122.74(5)^0. The reflection at 2θ = 24.62° (d = 3.61 Å), indicated by arrow in Figure 6a, which was indexed as the (010) peak corresponded to the $\pi-\pi$ interaction of closely stacked aromatic units, which is the typical $\pi-\pi$ stacking distance reported for OPV units in the literature.[37,38] The energy minimized conformation and length scale of both the OPVM-OH and UPBI-Py molecules were obtained with the help of DFT (B3LYP/6-31G (d.p.)) calculation, which are shown in SI Figure S7. OPVM-OH had the methacrylamide moiety out of plane of the three OPV rings and the length of the molecule in the plane from the $-CH_2$ to O−H was ∼19 Å. However, the indexed cell lengths in the ac plane were much bigger than the molecular length as derived from computational studies indicating a more complex structure possibly a centered one. The 1:1 complex [UPBI-Py (OPVM-OH)]$_{1.0}$ had peak pattern

that was different from that of the OPVM-OH (although peaks corresponding to UPBI-Py was more or less intact), especially in the region of 25−28° corresponding to stacking distances. $[UPBI\text{-}Py\ (OPVM\text{-}OH)]_{1.0}$ could be indexed to a monoclinic cell without taking into consideration the peaks from UPBI-Py. The cell parameters for the 1:1 complex $[UPBI\text{-}Py\ (OPVM\text{-}OH)]_{1.0}$ was a = 34.774(21), b = 4.537(3), c = 16.987(10), and β = 118.13(5)^0. The $\pi-\pi$ stacking distance increased to a d-spacing 4.537 Å corresponding to 2θ = 19.572° (dotted line in Figure 6a) in $[UPBI\text{-}Py\ (OPVM\text{-}OH)]_{1.0}$. The angle β, also changed from 122.74° in OPVM-OH to 118.13° in the 1:1 complex $[UPBI\text{-}Py\ (OPVM\text{-}OH)]_{1.0}$ indicating changes in the packing pattern upon complex formation. In order to further confirm the complex formation, two more complexes with varying mole ratios of the two molecules UPBI-Py and OPVM-OH were synthesized. They were $[UPBI\text{-}Py_{1.0}\ (OPVM\text{-}OH)_{2.0}]$ and $[UPBI\text{-}Py_{2.0}\ (OPVM\text{-}OH)_{1.0}]$. Figure 6b shows the stack plot of the normalized reflections of the three complexes expanded in the range 2θ = 3.5−35°. It could be seen that all three complexes exhibited complex peak pattern compared to the parent molecules indicating multiple phases. $[UPBI\text{-}Py_{2.0}\ (OPVM\text{-}OH)_{1.0}]$, which had higher molar ratio of UPBI-Py was less crystalline compared to the other complexes although the emergence of the crystalline peaks of the complex phase could be clearly observed. On the other hand, the $[UPBI\text{-}Py_{1.0}\ (OPVM\text{-}OH)_{2.0}]$ with higher molar ratio of OPVM-OH exhibited several sharp peaks that were not present in either OPVM-OH or UPBI-Py. An attempt was made to index these two complexes and the results in comparison with OPV and 1:1 complex are tabulated in Figure 6c. Distinct changes in the cell parameters could be discerned as OPVM-OH/UPBI-Py ratio changed in the complex clearly demonstrating the interaction existing between the two parent molecules UPBI-Py and OPVM-OH resulting in formation of new complexes.

The solid physical mixture of 1 mol each of UPBI-Py and OPVM-OH (prepared by mixing the powdered solid samples together), which was used earlier for the GPC experiments was studied for the WXRD reflections. Figure 7 compares the WXRD pattern of this mixture with that of OPVM-OH and UPBI-Py. Unlike the three complexes discussed previously, the

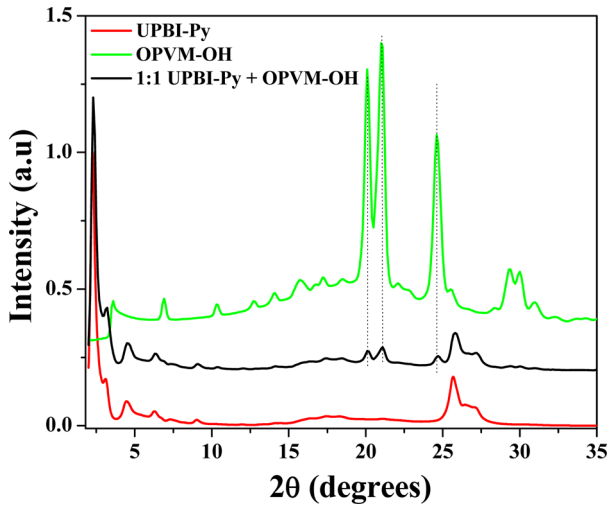

Figure 7. Wide angle X-ray diffraction pattern of OPVM-OH, UPBI-Py, and 1:1 physical mixture of OPVM-OH and UPBI-Py recorded at 25 °C (2θ from 2 to 35°).

solid physical mixture was a combination of reflections from both UPBI-Py and OPVM-OH and no shift was observed for the $\pi-\pi$ stacking reflection ~2θ = 24° suggesting that complexation had not occurred in the physical mixture.

Figure 8 compares the WXRD data of the supramolecular polymer $[UPBI\text{-}Py\ poly(OPVM\text{-}OH)]_{1.0}$ with that of the 1:1

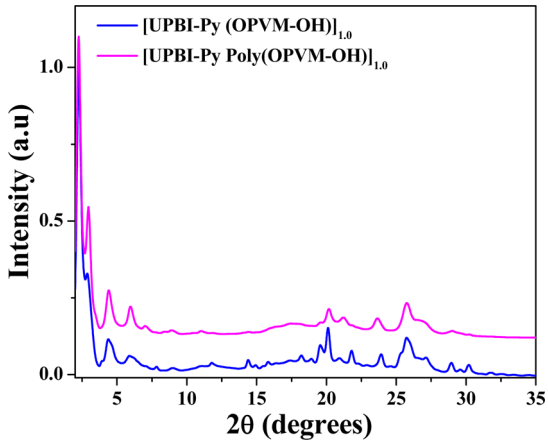

Figure 8. Wide angle X-ray diffraction pattern of $[UPBI\text{-}Py\ (OPVM\text{-}OH)]_{1.0}$ and supramolecular polymer complex $[UPBI\text{-}Py\ poly(OPVM\text{-}OH)]_{1.0}$ recorded at 25 °C (2θ from 2 to 35°).

complex $[UPBI\text{-}Py\ (OPVM\text{-}OH)]_{1.0}$. An overall reduction in crystallinity was observed in the polymer compared to the 1:1 complex. This could be attributed to the presence of the flexible methacrylate polymer backbone. The Supporting Information (Figure S8−11; ST-1a−f) gives the indexed figure as well as the entire Bragg reflections and their corresponding d spacings for the donor, acceptor, the supramolecular polymer, as well as the various complexes.

Thin Film Morphology. Thin film morphology of the complex and supramolecular polymer were analyzed using transmission electron microscopy (TEM). The 1:1 OPV:PBI complex was drop cast (2 mg/mL DMF solution) onto the copper grid and subjected to selective staining using Osmium tetroxide (OsO_4).[39] Striated nanostructure in the length scale of <10 nm formed by the lamellar structure of the complex was observed covering large area of the grid as shown in Figure 9a−c. The dark lines corresponded to OPV layers stained by OsO_4 while the bright lines corresponded to those of crystalline perylene units. The statistically averaged thickness of the dark and bright region measured from the TEM image using the instrument software was ~18 Å (SI Figure S12m). The starting materials OPVM-OH and UPBI-Py did not exhibit any characteristic morphology under identical conditions. SI Figure S12a−c and S12d−f shows the TEM images of drop cast samples of OPVM-OH and UPBI-Py on TEM grids. Therefore, it was obvious that the donor (OPV) and acceptor (PBI) had formed well developed alternating parallel nanostructured lamellae as a result of the self-assembly. There are reports in literature on the large area self-assembly of small organic molecules where the self-assembly in solution was translated in thin films upon processing.[40,41] Hydrogen bond directed supramolecular self-assembly between oligo(*p*-phenylenevinylenes) containing ureidotriazine and perylene bisimide were shown to form lamellar structures as well as chiral stacks.[42−44] The thin film morphology of the polymer formed by thermal polymerization as well as photopolymerization was also

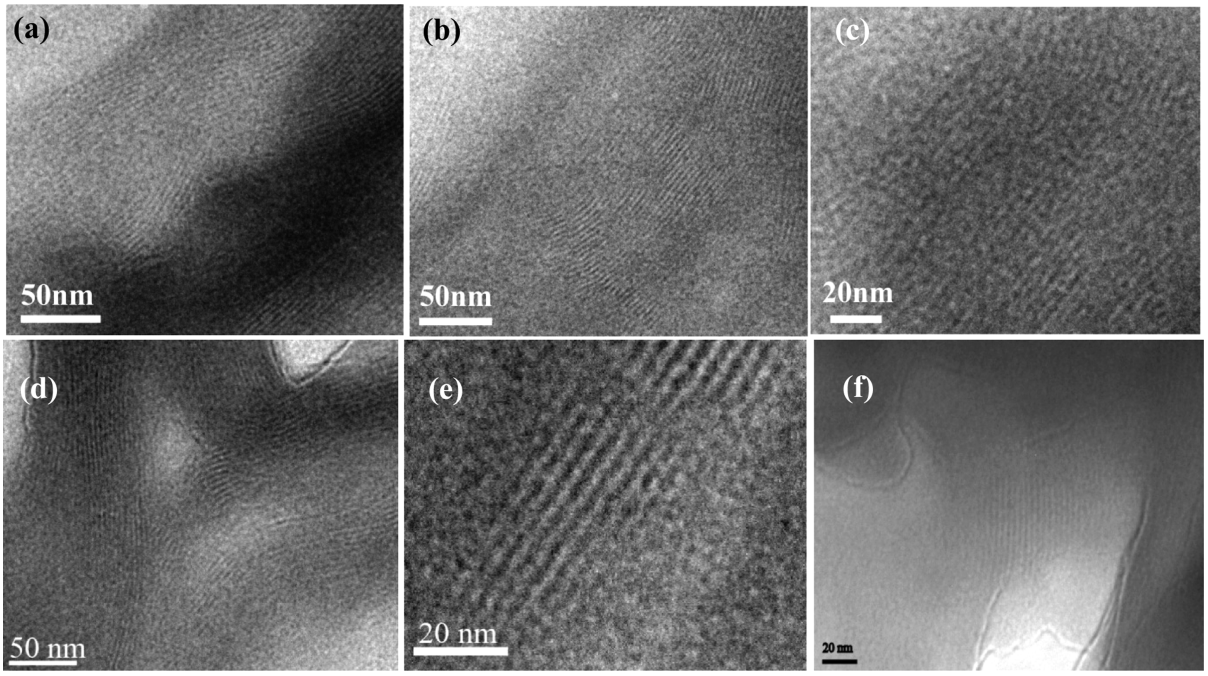

Figure 9. TEM images (samples drop cast from DMF solution at 2 mg/mL concentration) of (a–c) 1:1 complex $[UPBI\text{-}Py\ (OPVM\text{-}OH)]_{1.0}$ and (d–f) supramolecular polymer complex $[UPBI\text{-}Py\ poly(OPVM\text{-}OH)]_{1.0}$ at different length scale, recorded at room temperature.

analyzed using TEM. Figure 9d–f shows the images for the supramolecular polymer which was stained using OsO_4. Beautiful lamellar striations were visible covering large area of the grid for the supramolecular polymer complex also. The average thickness of the bright and dark area determined using the instrument software was ~18 Å (SI Figure S12n). The length scale of ~18 Å observed in the TEM images correlated very well with the molecular length of UPBI-Py and OPVM-OH obtained using DFT (B3LYP/6-31G (d.p.)) calculation (SI Figure S7).

Electron Mobility and Photoconductivity Studies. The charge carrier mobility in the small molecule UPBI-Py, the 1:1 D–A supramolecular complex $[UPBI\text{-}Py\ (OPVM\text{-}OH)]_{1.0}$ and the D–A supramolecular polymer complex $[UPBI\text{-}Py\ poly(OPVM\text{-}OH)]_{1.0}$ was evaluated using space charge limited current (SCLC) measurements. The current voltage characteristics of the devices made were measured in dark as well as under illumination. Space charge regime in $J(V)$ was observed in $[UPBI\text{-}Py\ (OPVM\text{-}OH)]_{1.0}$ and $[UPBI\text{-}Py\ poly(OPVM\text{-}OH)]_{1.0}$ for the devices tested and mobility was estimated from $J(V)$ relationship measured under dark condition. Table 1 summarizes the device parameters, and SI Figure S13 gives the photo current vs bias voltage curve of the samples. The pristine UPBI-Py exhibited SCLC with a bulk mobility estimate of $\approx 10^{-4}$ cm^2 V^{-1} s^{-1} whereas the mobility estimate was an order higher for $[UPBI\text{-}Py\ (OPVM\text{-}OH)]_{1.0} \sim 10^{-3}$ cm^2 V^{-1}s^{-1}. The polymer complex $[UPBI\text{-}Py\ poly(OPVM\text{-}OH)]_{1.0}$ exhibited mobility $\approx 10^{-4}$ cm^2 V^{-1} s^{-1}. The intensity dependence of the photocurrent response of these samples also reveal interesting trends with a superlinear response in case of D–A complex and poly(D-A) complex. Figure 10 compares the photocurrent response of UPBI-Py, $[UPBI\text{-}Py\ (OPVM\text{-}OH)]_{1.0}$, and $[UPBI\text{-}Py\ poly(OPVM\text{-}OH)]_{1.0}$ and Table 2 lists the maximum mobility $\mu_{e,max}$ (cm^2/(V s)) under irradiation at two different light intensities. Higher photocurrent response was observed for UPBI-Py $(OPVM\text{-}OH)]_{1.0}$ and $[UPBI\text{-}Py\ poly(OPVM\text{-}OH)]_{1.0}$ with high responsivity (≈ 1 μA/W) compared to the pristine acceptor UPBI-Py device. The higher photocurrent could be attributed to the facile photoinduced charge generation and separation factors prevailing in the D–A system. The network required for independent electron and hole transport however is constrained leading to sizable

Table 1. Summary of Device Parameters

sample	maximum mobility $\mu_{e,max}$ (cm^2/(V s))	average mobility $\mu_{e,avg}$ (cm^2/(V s))	mean deviation
UPBI-Py	2.08×10^{-4}	1.62×10^{-4}	$\pm 4 \times 10^{-5}$
$[UPBI\text{-}Py\ (OPVM\text{-}OH)]_{1.0}$	8×10^{-3}	7×10^{-3}	$\pm 5 \times 10^{-4}$
$[UPBI\text{-}Py\ poly(OPVM\text{-}OH)]_{1.0}$	6.2×10^{-4}	5.11×10^{-4}	$\pm 9 \times 10^{-5}$

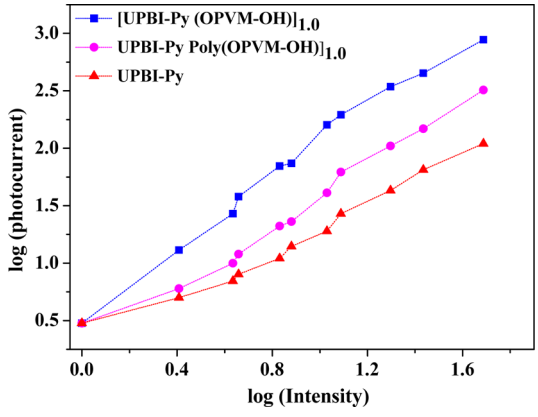

Figure 10. Photoconductive characterization upon irradiation with increasing power density at −2 V bias (normalized photocurrent in pA and Intensity in mW/cm^2).

Table 2. Photoconductivity Characterization in the Dark and under White Light Irradiation of Increasing Intensity

sample	max. mobility $\mu_{e,max}$ ($cm^2/(V\ s)$) (in dark)	max. mobility $\mu_{e,max}$ ($cm^2/(V\ s)$) (under irradiation; intensity 0.2 mW/cm^2)	max. mobility $\mu_{e,max}$ ($cm^2/(V\ s)$) (under irradiation; intensity 1.1 mW/cm^2)	responsivity (nA/W)
UPBI-Py	2.08×10^{-4}	4.53×10^{-4}	1.13×10^{-3}	10
$[\text{UPBI-Py (OPVM-OH)}]_{1.0}$	8×10^{-3}	2.4×10^{-2}	5.4×10^{-2}	1000
$[\text{UPBI-Py poly(OPVM-OH)}]_{1.0}$	6.2×10^{-4}	1.7×10^{-4}	4.57×10^{-3}	100

trapping and recombination losses, and can be the cause for the superlinear intensity dependence. Additionally, the presence of the insulating methacrylate polymer backbone in case of the supramolecular D−A polymer complex could also lower the mobility and photocurrent magnitude compared to the observed trends in case of the D−A complex. In short, the observed trend in the different systems provides a guide toward design of appropriate D−A building blocks for efficient optoelectronic properties.

CONCLUSION

In conclusion, we have shown that donor and acceptor small molecules based on complementarily functionalized oligo(*p*-phenylenevinylene) (OPVM-OH) and N-substituted perylene-bisimide (UPBI-Py) for hydrogen bonding interactions could be organized into lamellar structures in the domain range 5 to 10 nm using the concept of supramolecular assembly. A 1:1 supramolecular complex of OPVM-OH and UPBI-Py was prepared, structurally characterized and further subjected to polymerization thermally as well as by photo irradiation resulting in supramolecular donor−acceptor complex polymer. The homopolymer of the donor alone without complexation with the acceptor UPBI-Py resulted in an insoluble polymer which could not be fully characterized. Complexation improved the solubility of the donor−acceptor polymer by several folds. The emission from thin drop cast films of the 1:1 donor−acceptor complex was considerably quenched compared to the donor alone or acceptor alone thin film samples. The emission spectra of thin film samples of the supramolecular polymer complex exhibited subtle organizational changes occurring in the donor (OPV) emission upon its polymerization. Compared to the red-shifted aggregate emission from OPV observed in $[\text{UPBI-Py (OPVM-OH)}]_{1.0}$, the supramolecular polymer $[\text{UPBI-Py poly(OPVM-OH)}]_{1.0}$ exhibited monomeric OPV emission indicating that the self-assembly of OPV was disrupted upon polymerization due to the formation of methacrylamide linkage in the backbone. Solid state measurements such as FTIR and WXRD and thin film morphology using TEM were undertaken to understand the self-organization. WXRD studies showed that donor−acceptor complex formation between UPBI-Py and OPVM-OH resulted in distinct changes in the cell parameters of OPVM-OH. Polymerization of the donor within the supramolecular D−A complex resulted in a reduction in overall crystallinity in the supramolecular complex polymer. Photo response measurements of the D−A supramolecular complex indicated a clear trend of higher conductance compared to pristine UPBI-Py. This is the first time that such superior lamellar organization of the donor and acceptor organic semiconducting molecules has been achieved without the aid of a templating polymer or block copolymer. The highlight of this approach was the improved processability afforded by the improved solubility of the D−A supramolecular complex compared to the donor or acceptor alone, while at the same time maintaining the crystalline organization also. This concept is extendable to the analogous complementarily functionalized donor−acceptor pairs (such as oligothiophene and perylene/naphthalene bisimides), which can be further polymerized in order to facilitate processability. Work along this line is in progress currently.

ASSOCIATED CONTENT

Supporting Information

Experimental procedure and characterization of OPVM-OH and UPBI-Py. Characterization of 1:1 complex $[\text{UPBI-Py (OPVM-OH)}]_{1.0}$ and supramolecular polymer complex $[\text{UPBI-Py poly(OPVM-OH)}]_{1.0}$. Thin film morphology (TEM images) of OPM-OH, UPBI-Py, 1:1 complex $[\text{UPBI-Py (OPVM-OH)}]_{1.0}$ including other two complexes named as $[\text{UPBI-Py}_{1.0}\ (\text{OPVM-OH})_{2.0}]$, $[\text{UPBI-Py}_{2.0}\ (\text{OPVM-OH})_{1.0}]$, and supramolecular polymer complex $[\text{UPBI-Py poly(OPVM-OH)}]_{1.0}$. Photo current vs bias voltage curve of three samples. This material is available free of charge via the Internet at http://pubs.acs.org.

AUTHOR INFORMATION

Corresponding Authors

*E-mail: narayan@jncasr.ac.in. PABX: 220-82750.
*E-mail: sk.asha@ncl.res.in. Fax: 0091-20-25902615.

Notes

The authors declare no competing financial interest.

ACKNOWLEDGMENTS

This work has been financially supported by the network project NWP0054 and DST Nano Mission project SR/NM/NS-1028/2012. The authors thank Mr. Pankaj Sankapalli, NCL−Pune for TEM imaging, Mr. Yogesh N Marathe for the WXRD measurements and Ms. Chayanika Das for the DFT (B3LYP/6-31G(d.p.)) studies. Saibal thanks UGC-New Delhi, India for Senior Research Fellowship.

REFERENCES

(1) Aida, T.; Meijer, E. W.; Stupp, S. I. Functional Supramolecular Polymers. *Science* **2012**, *335*, 813−817.
(2) Neuteboom, E. E.; Meskers, S. C. J.; Van Hal, P. A.; Van Duren, J. K. J.; Meijer, E. W.; Janssen, R. A. J.; Dupin, H.; Pourtois, G.; Cornil, J.; Lazzaroni, R.; Brédas, J.-L.; Beljonne, D. Alternating Oligo(*p*-phenylene vinylene)−Perylene Bisimide Copolymers: Synthesis, Photophysics, and Photovoltaic Properties of a New Class of Donor−Acceptor Materials. *J. Am. Chem. Soc.* **2003**, *125*, 5174−5176.
(3) Jalani, K.; Kumar, M.; George, S. J. Mixed Donor−Acceptor Charge-Transfer Stacks Formed via Hierarchical Self-Assembly of a Non-Covalent Amphiphilic Foldamer. *Chem. Commun.* **2013**, *49*, 14968−14969.
(4) Park, B.; Cho, S. E.; Kim, Y.; Lee, W. J.; You, N.-H.; In, I.; Reichmanis, E. Simultaneous Study of Exciton Diffusion/Dissociation and Charge Transport in a Donor-Acceptor Bilayer: Pentacene on a

C_{60}-terminated Self-Assembled Monolayer. *Adv. Mater.* **2013**, *25*, 6453−6458.
(5) Aiyar, A. R.; Hong, Jung-Il.; Izumi, J.; Choi, D.; Kleinhenz, N.; Reichmanis, E. Ultrasound-Induced Ordering in Poly(3-hexylthiophene): Role of Molecular and Process Parameters on Morphology and Charge Transport. *ACS Appl. Mater. Interfaces* **2013**, *5*, 2368−2377.
(6) De Boer, B.; Stalmach, U.; van Hutten, P. F.; Melzer, C.; Krasnikov, V. K.; Hadziioannou, G. Supramolecular Self-Assembly and Opto-Electronic Properties of Semiconducting Block Copolymers. *Polymer* **2001**, *42*, 9097−9109.
(7) Mativetsky, J. M.; Kastler, M.; Savage, R. C.; Gentilini, D.; Palma, M.; Pisula, W.; Müllen, K.; Samorí, P. Self-Assembly of a Donor−Acceptor Dyad Across Multiple Length Scales: Functional Architectures for Organic Electronics. *Adv. Funct. Mater.* **2009**, *19*, 2486−2494.
(8) Zapala, J.; Knor, M.; Jaroch, T.; Maranda-Niedbala, A.; Kurach, E.; Kotwica, K.; Nowakowski, R.; Djurado, D.; Pecaut, J.; Zagorska, M.; Pron, A. Self-Assembly Properties of Semiconducting Donor−Acceptor−Donor Bithienyl Derivatives of Tetrazine and Thiadiazole—Effect of the Electron Accepting Central Ring. *Langmuir* **2013**, *29*, 14503−14511.
(9) Ikkala, O.; ten Brinke, G. Functional Materials Based on Self-Assembly of Polymeric Supramolecules. *Science* **2002**, *295*, 2407−2409.
(10) Hanski, S.; Houbenov, N.; Ruokolainen, J.; Chondronicola, D.; Iatrou, H.; Hadjichristidis, N.; Ikkala, O. Hierarchical Ionic Self-Assembly of Rod−Comb Block Copolypeptide−Surfactant Complexes. *Biomacromolecules* **2006**, *7*, 3379−3384.
(11) Ruokolainen, J.; Mäkinen, R.; Torkkeli, M.; Mäkelä, T.; Serimaa, R.; ten Brinke, G.; Ikkala, O. Switching Supramolecular Polymeric Materials with Multiple Length Scales. *Science* **1998**, *280*, 557−560.
(12) Ruokolainen, J.; ten Brinke, G.; Ikkala, O.; Torkkeli, M.; Serimaa, R.; Komanschek, E. Order-Disorder Transitions in Polymer−Surfactant Systems. *Phys. Rev. E* **1996**, *54*, 6646−6649.
(13) Narayan, R.; Kumar, P.; Narayan, K. S.; Asha, S. K. Nanostructured Crystalline Comb Polymer of Perylenebisimide by Directed Self-Assembly: Poly(4-vinylpyridine)-pentadecylphenol Perylenebisimide. *Adv. Funct. Mater.* **2013**, *23*, 2033−2043.
(14) Rancatore, B. J.; Mauldin, C. E.; Fréchet, J. M. J.; Xu, T. Small Molecule-Guided Thermoresponsive Supramolecular Assemblies. *Macromolecules* **2012**, *45*, 8292−8299.
(15) Rancatore, B. J.; Mauldin, C. E.; Tung, S. H.; Wang, C.; Hexemer, A.; Strzalka, J.; Fréchet, J. M.J.; Xu, T. Nanostructured Organic Semiconductors via Directed Supramolecular Assembly. *ACS Nano* **2010**, *4*, 2721−2729.
(16) Perepichka, I. I.; Lu, Q.; Badia, A.; Bazuin, C. G. Understanding and Controlling Morphology Formation in Langmuir-Blodgett Block Copolymer Films Using PS-P4VP and PS- P4VP/PDP. *Langmuir* **2013**, *29*, 4502−4519 29, 4502−4519.
(17) Hu, H.; Gopinadhan, M.; Osuji, C. O. Directed Self-Assembly of Block Copolymers: A Tutorial Review of Strategies for Enabling Nanotechnology with. *Soft Matter* **2014**, *10*, 3867−3889.
(18) Cummins, C.; Borah, D.; Rasappa, S.; Chaudhari, A.; Ghoshal, T.; O'Driscoll, B. M. D.; Carolan, P.; Petkov, N.; Holmes, J. D.; Morris, M. A. Self-Assembly of Polystyrene-*block*-Poly(4-vinylpyridine) Block Copolymer on Molecularly Functionalized Silicon Substrates: Fabrication of Inorganic Nanostructured Etchmask for Lithographic Use. *J. Mater. Chem. C* **2013**, *1*, 7941−7951.
(19) Kao, J.; Thorkelsson, K.; Bai, P.; Rancatore, B. J.; Xu, T. Toward Functional Nanocomposites: Taking the Best of Nanoparticles, Polymers, and Small Molecules. *Chem. Soc. Rev.* **2013**, *42*, 2654−2678.
(20) Thorkelsson, K.; Mastroianni, A. J.; Ercius, P.; Xu, T. Direct Nanorod Assembly Using Block Copolymer-Based Supramolecules. *Nano Lett.* **2012**, *12*, 498−504.
(21) Ruokolainen, J.; ten Brinke, G.; Ikkala, O. Supramolecular Polymeric Materials with Hierarchical Structure-Within-Structure Morphologies. *Adv. Mater.* **1999**, *11*, 777−780.
(22) van Zoelen, W.; van Ekenstein, G. A.; Polushkin, E.; Ikkala, O.; ten Brinke, G. Nanorod Engineering by Reinforcing Hexagonally Self-Assembled PS-*b*-P4VP(DDP) with PPE. *Soft Matter* **2005**, *1*, 280−283.
(23) Ono, R. J.; Todd, A. D.; Hu, Z.; Vanden Bout, D. A.; Bielawski, C. W. Synthesis of a Donor−Acceptor Diblock Copolymer via Two Mechanistically Distinct, Sequential Polymerizations Using a Single Catalyst. *Macromol. Rapid Commun.* **2014**, *35*, 204−209.
(24) Wang, J.; Higashihara, T. Synthesis of All-Conjugated Donor−Acceptor Block Copolymers and Their Application in All-Polymer Solar Cells. *Polym. Chem.* **2013**, *4*, 5518−5526.
(25) You, C.-C.; Würthner, F. Self-Assembly of Ferrocene-Functionalized Perylene Bisimide Bridging Ligands with Pt(II) Corner to Electrochemically Active Molecular Squares. *J. Am. Chem. Soc.* **2003**, *125*, 9716−9725.
(26) Lane, T. J.; Nakagawa, I.; Walter, J. L.; Kandathil, A. J. Infrared Investigation of Certain Imidazole Derivatives and Their Metal Chelates. *Inorg. Chem.* **1962**, *1*, 267−276.
(27) Moussa, K.; Decker, C. Light-Induced Polymerization of New Highly Reactive Acrylic Monomers. *J. Polym. Sci. Part A: Polym. Chem.* **1993**, *31*, 2197−2203.
(28) Rekha, N.; Asha, S. K. Synthesis and FTIR Spectroscopic Investigation of the UV Curing Kinetics of Telechelic Urethane Methacrylate Crosslinkers Based on the Renewable Resource—Cardanol. *J. Appl. Polym. Sci.* **2008**, *109*, 2781−2790.
(29) Schenning, A. P. H. J.; Peeters, E.; Meijer, E. W. Energy Transfer in Supramolecular Assemblies of Oligo(*p*-phenylene vinylene)s Terminated Poly(propylene imine) Dendrimers. *J. Am. Chem. Soc.* **2000**, *122*, 4489−4495.
(30) Shao, C.; Grüne, M.; Stolte, M.; Würthner, F. Perylene Bisimide Dimer Aggregates: Fundamental Insights into Self-Assembly by NMR and UV/Vis Spectroscopy. *Chem.—Eur. J.* **2012**, *18*, 13665−13677.
(31) Draper, E. R.; Walsh, J. J.; McDonald, T. O.; Zwijnenburg, M. A.; Cameron, P. J.; Cowan, A. J.; Adams, D. J. Air-Stable Photoconductive Films Formed From Perylene Bisimide Gelators. *J. Mater. Chem. C* **2014**, *2*, 5570−5575.
(32) Chen, Z.; Stepanenko, V.; Dehm, V.; Prins, P.; Siebbeles, L. D. A.; Seibt, J.; Marquetand, P.; Engel, V.; Würthner, F. Photoluminescence and Conductivity of Self-Assembled $\pi-\pi$ Stacks of Perylene Bisimide Dyes. *Chem.—Eur. J.* **2007**, *13*, 436−449.
(33) Zhang, J.; Hoeben, F. J. M.; Pouderoijen, M. J.; Schenning, A. P.; Meijer, E. W.; De Schryver, F. C.; De Feyter, S. Hydrogen-Bonded Oligo(*p*-phenylene vinylene) Functionalized with Perylene Bisimide: Self-Assembly and Energy Transfer. *Chem.—Eur. J.* **2006**, *12*, 9046−9055.
(34) van Hutten, P. F.; Brouwer, H.-J.; Krasnikov, V. V.; Ouali, L.; Stalmach, U.; Hadziioannou, G. Effect of Solid-State Structure on Optical Properties of Conjugated Organic Materials. *Synth. Met.* **1999**, *102*, 1443−1446.
(35) Ramakrishna Matte, H. S. S.; Jain, A.; George, S. J. Covalently Linked Graphene-Oligo(phenylene vinylene) Adduct: Self Organization and Photo-physical Properties. *RSC Adv.* **2012**, *2*, 6290−6294.
(36) Samuel, I. D.W.; Rumbles, G.; Collison, C. Efficient Interchain Photoluminescence in a High-Electron-Affinity Conjugated Polymer. *Phys. Rev. B* **1995**, *52*, RII573−RII 576.
(37) George, S. J.; Ajayaghosh, A. Self-Assembled Nanotapes of Oligo(*p*-phenylene vinylene)s: Sol−Gel-Controlled Optical Properties in Fluorescent π-Electronic Gels. *Chem.—Eur. J.* **2005**, *11*, 3217−3227.
(38) Hutten, P. F. V.; Krasnikov, V. V.; Hadziioannou, G. A. Model Oligomer Approach to Light-Emitting Semiconducting Polymers. *Acc. Chem. Res.* **1999**, *32*, 257−265.
(39) Brochon, C.; Sary, N.; Mezzenga, R.; Ngov, C.; Richard, F.; May, M.; Hadziioannou, G. Synthesis of Poly(*p*-phenylene vinylene)—Polystyrene-Based Rod-Coil Block Copolymer by Atom Transfer Radical Polymerization: Toward a Self-Organized Lamellar Semiconducting Material. *J. Appl. Polym. Sci.* **2008**, *110*, 3664−3670.
(40) De Luca, G.; Liscio, A.; Battagliarin, G.; Chen, L.; Scolaro, L. M.; Müllen, K.; Samorì, P.; Palermo, V. Orthogonal Self-Assembly and Selective Solvent Vapour Annealing: Simplified Processing of a Photovoltaic Blend. *Chem. Commun.* **2013**, *49*, 4322−4324.

(41) Ciesielski, A.; Szabelski, P.; Cadeddu, A.; Cook, T. R.; Stang, P. J.; Samorì, P. Concentration-Dependent Supramolecular Engineering of Hydrogen-Bonded Nanostructures at Surfaces: Predicting Self-Assembly in 2D. *J. Am. Chem. Soc.* **2013**, *135*, 6942−6950.
(42) Schenning, A. P. H. J.; van Herrikhuyzen, J.; Jonkheijm, P.; Chen, Z.; Würthner, F.; Meijer, E. W. Photoinduced Electron Transfer in Hydrogen-Bonded Oligo(*p*-phenylene vinylene)−Perylene Bisimide Chiral Assemblies. *J. Am. Chem. Soc.* **2002**, *124*, 10252−10253.
(43) Würthner, F.; Chen, Z.; Hoeben, F. J. M.; Osswald, P.; You, C.-C.; Jonkheijm, P.; van Herrikhuyzen, J.; Schenning, A. P. H. J.; Schoot, P. P. A. M. v. d.; Meijer, E. W.; Beckers, E. H. A.; Meskers, S. C. J.; Janssen, R. A. J. Supramolecular p-n Heterojunctions by Co-Self-Organization of Oligo(*p*-phenylene vinylene) and Perylene Bisimide Dyes. *J. Am. Chem. Soc.* **2004**, *126*, 10611−10618.
(44) Pascal, J.; Stutzmann, N.; Chen, Z.; de Leeuw, D. M.; Meijer, E. W.; Schenning, A. P. H. J.; Würthner, F. Control of Ambipolar Thin Film Architectures by Co-Self-Assembling Oligo(*p*-phenylene vinylene)s and Perylene Bisimides. *J. Am. Chem. Soc.* **2006**, *128*, 9535−9540.